

# Interplay Between Interference-Aware Resource Allocation Algorithm Design, CSI, and Feedback in Underlay D2D Networks

Bala Venkata Ramulu Gorantla<sup>1</sup>, *Student Member, IEEE*, and Neelesh B. Mehta<sup>2</sup>, *Fellow, IEEE*

**Abstract**—A key problem in underlay device-to-device (D2D) systems is assigning cellular users and D2D users to subchannels to improve spatial reuse while controlling the interference they cause to each other. We present a unified treatment of this problem for two practically motivated partial and statistical channel state information (CSI) models with quantized feedback. They differ in the CSI available at the D2D receiver. In both models, the nodes only have statistical information of inter-D2D and inter-cell interferences, and employ fractional power control. We present two polynomial-time algorithms to assign multiple D2D pairs to subchannels, namely, relaxation-pruning algorithm (RPA) and cardinality-constrained subchannel assignment algorithm (CCSAA). RPA and CCSAA guarantee a D2D sum rate that is at least one-half and one-third, respectively, of the optimal sum rate. We also propose a novel statistical rate upgradation technique that exploits the allocation information to improve the D2D rates. We observe that inter-D2D interference has a more pronounced effect in the statistical CSI model. The algorithms respond differently to the two CSI models. RPA outperforms CCSAA in the partial CSI model, while CCSAA outperforms RPA in the statistical CSI model despite its weaker performance guarantee.

**Index Terms**—D2D, subchannel allocation, channel state information, quantized feedback, inter-cell interference, inter-D2D interference.

## I. INTRODUCTION

5G PROMISES to offer a wide variety of services and applications that connect many devices with high data rates. It enables an exciting class of new proximity services (ProSe), such as local social-networking, local advertising, first-responder communications, vehicle-to-vehicle communications, and video caching. Device-to-device (D2D) communication enables these services. In it, devices communicate directly with each other without routing their data through the base station (BS). Doing so improves spatial reuse, energy

efficiency, and latency. Standardization activities are actively being pursued in 3GPP to specify the D2D use cases and protocols [2]. D2D is also being considered in combination with other technologies such as non-orthogonal multiple access [3].

In underlay D2D communication, the D2D users share subchannels with the cellular users (CUs) to improve spatial reuse. However, this causes the CUs and the D2D users to interfere with each other. For example, in the uplink, the CU causes interference to the D2D receiver (DRx) while the D2D transmitter (DTx) causes interference to the BS. Therefore, interference-aware subchannel allocation algorithms are essential at the BS to provide quality-of-service (QoS) guarantees to the CUs and improve spectral efficiency.

The design and efficacy of the resource allocation algorithm depends on the channel state information (CSI) available at the BS and D2D pairs. For example, the full CSI models of [4]–[9] assume that the BS knows with infinite precision the channel gains of all the CU-to-BS, CU-to-DRx, DTx-to-BS, and DTx-to-DRx links in the system. These models are practically untenable because the DTx-to-DRx and CU-to-DRx channel gains need to be fed back to the BS by the D2D users. This makes models in which the BS only has limited CSI about the DTx-to-DRx links and/or the CU-to-DRx links very appealing.

### A. Literature Survey on D2D With Limited CSI

We now summarize the D2D literature that considers limited CSI. We classify them below on the basis of the CSI the BS has and whether one or multiple D2D pairs can share a subchannel.

1) *One D2D Pair per Subchannel*: In [10], subchannel and power allocation to the D2D pairs and CUs is first carried out assuming that the BS has only statistical CSI of the CU-to-DRx links. Another model in which each DRx feeds back to the BS the CSI of the interference links from a pre-specified number of farthest CUs is also studied. The problem is solved using the polynomial-time Kuhn-Munkres algorithm. The same algorithm is used in [11] for the statistical CSI model. In [12], a partial CSI model is assumed in which the BS receives one-bit feedback from the DRx for each of its links to the CUs. A polynomial-time, throughput-optimal algorithm is proposed for joint user scheduling, D2D mode selection, and discrete rate adaptation. A dynamic mode selection scheme based on the received signal strength from the BS is considered

Manuscript received February 3, 2021; revised May 11, 2021, July 6, 2021, and August 29, 2021; accepted October 12, 2021. Date of publication October 28, 2021; date of current version May 10, 2022. An earlier version of this paper was presented in part at the IEEE International Conference on Communications (ICC), in June 2021, [DOI: 10.1109/ICC42927.2021.9500968]. The associate editor coordinating the review of this article and approving it for publication was X. Chen. (*Corresponding author: Bala Venkata Ramulu Gorantla.*)

The authors are with the Department of Electrical Communication Engineering (ECE), Indian Institute of Science (IISc), Bengaluru 560012, India (e-mail: balavenkataramulu@gmail.com; nbmehta@iisc.ac.in).

Color versions of one or more figures in this article are available at <https://doi.org/10.1109/TWC.2021.3121874>.

Digital Object Identifier 10.1109/TWC.2021.3121874

in [13] to manage the interference from a D2D user to the CU link. In [14], a statistical CSI model is considered for a multi-cell scenario with only one CU and D2D pair. A heuristic two-step algorithm is proposed to determine the transmit powers of the CU and D2D pair. In [15], for the statistical CSI model, subchannel and power allocation of the D2D pairs is done to improve the energy efficiency of the CUs and D2D pairs while guaranteeing the D2D pairs a minimum rate with a pre-specified probability of outage.

2) *Multiple D2D Pairs per Subchannel*: In [16], for the statistical CSI model, a heuristic algorithm for allocating subchannels is proposed that clusters the CUs and D2D pairs. In [17], for the statistical CSI model, a distributed admission control method for the D2D pairs is proposed for a multi-cell scenario in which each cell has only one CU and multiple D2D pairs, and all of them reuse the same subchannel. In [18], the DRx feeds back a quantized version of its signal-to-interference-plus-noise ratio (SINR) to the BS. A polynomial-time algorithm called cardinality-constrained subchannel assignment algorithm (CCSAA) is proposed for allocating subchannels to the D2D pairs while ensuring a minimum rate with a pre-specified probability of outage for the CUs. It guarantees a D2D sum rate that is at least one-third of the optimal sum rate. In [19], D2D pairs that share the same subchannel are grouped into clusters. A topological interference management scheme is proposed to maximize the number of parallel interference-free links within the cluster.

Resource allocation with imperfect estimates of the CU-to-DRx and DTx-to-DRx channel gains is considered in [20]–[22]. However, only one subchannel is considered in [20], [21]. In [22], a multi-objective optimization investigates the trade-off between spectral-efficiency and energy-efficiency for a bounded estimation error model.

We see that even for the limited CSI models, the above papers differ in their consideration of inter-cell interference, the number of D2D pairs allocated to a subchannel, and the number of subchannels. Table I summarizes how the literature differs in these aspects.

## B. Focus and Contributions

We investigate the problem of allocating one or more D2D pairs per subchannel for an underlay D2D system with multiple subchannels, CUs, and D2D pairs. We do this in a unified manner for two practical CSI models. We make the following contributions:

1) *Two Practically Relevant CSI Models*: We consider a *partial CSI model* and a *statistical CSI model*. In both models, the DRx knows the statistics of the inter-cell and inter-D2D interferences, but not their instantaneous values. In the partial CSI model, the DRx knows the instantaneous channel gains of its DTx-to-DRx and CU-to-DRx links. This is applicable when the DRx periodically measures transmissions from the DTx and the CU. In the statistical CSI model, the DRx only has statistical CSI of the DTx-to-DRx and CU-to-DRx links. This is applicable when the DRx measures the channel gains infrequently.

2) *Quantized Feedback Design With Outage Guarantees*: For both models, the DRx feeds back a  $q$ -bit quantized esti-

mate of its SINR, where  $q$  is a system parameter that controls signaling overhead. Despite the limited CSI, the feedback is such that the rate achieved using it can be decoded with an outage probability of at most  $\epsilon_d$ .

3) *Polynomial-Time Algorithms With Performance Guarantees*: For both CSI models, the problem of allocating multiple D2D pairs to multiple subchannels turns out to be NP-hard. To solve it, we propose two polynomial-time algorithms that employ markedly different approaches. The first one is a novel relaxation-pruning algorithm (RPA). It is an adaptation of the Shmoys and Tardos algorithm [23]. RPA provably achieves a D2D sum rate that is at least half of the optimal D2D sum rate. The second one is CCSAA. It is a combination of the Goundan-Schulz algorithm [24] and an algorithm by Caprara et al. [25] for the cardinality-constrained knapsack problem. CCSAA has a lower computational complexity and provably achieves a D2D sum rate that is at least one-third of the optimal D2D sum rate. Both algorithms allocate at most  $K$  D2D pairs per subchannel, where  $K$  is a system parameter that controls the inter-D2D interference. They also guarantee a minimum rate with a pre-specified probability of outage  $\epsilon_c$  for the CUs.

4) *Novel Statistical Rate Upgradation (SRU) Technique*: We propose a technique called SRU that enables the D2D pairs to increase their data rate. It exploits the information broadcast by the BS about the allocation of the D2D pairs to the subchannels to determine accurately the statistics of the inter-D2D interference. SRU significantly improves the D2D sum rate.

5) *Interplay Between CSI Model, Feedback Resolution, and Algorithm Design*: Our comprehensive numerical results bring out several novel insights about the interplay between the CSI model, algorithm design, and feedback. First, RPA outperforms CCSAA for the partial CSI model. However, CCSAA outperforms RPA for the statistical CSI model despite offering a weaker performance guarantee. In effect, RPA is better able to exploit the larger variation in the rates across subchannels that occurs for the partial CSI model. Second, inter-D2D interference has a more pronounced effect in the statistical CSI model than the partial CSI model. Third, the optimal value of  $K$  depends on the CSI model, feedback resolution, and algorithm.

## C. Comparison With Literature

Our work differs from the literature in numerous respects. First, we do not assume full CSI [4]–[8] due to the large feedback overhead it entails. Second, inter-cell interference is not considered in [10], [11], [15], [16], [19]. Thus, its randomness and the uncertainty it causes in the SINRs and rates is not addressed in these papers. Third, quantized feedback, which is inevitable in practice, is not considered in the literature except for [12], [18]. Fourth, only one D2D pair is allocated per subchannel in [10]–[12], [14], [15]. The problem of assigning multiple D2D pairs per subchannel in a system with multiple subchannels is fundamentally different and more involved than considering only one subchannel or assigning at most one D2D pair per subchannel. Unlike the

TABLE I  
COMPARISON OF LITERATURE ON RESOURCE ALLOCATION IN D2D NETWORKS WITH LIMITED CSI

Reference	D2Ds per subchannel	Subchannels	Inter-cell interference	CSI at BS
Feng et al. [10] (Model 1)	Single	Multiple	No	DTx-DRx (instantaneous), CU-DRx (instantaneous)
Feng et al. [10] (Model 2)	Single	Multiple	No	DTx-DRx (instantaneous), CU-DRx (statistical)
Wang et al. [11]	Single	Multiple	No	DTx-DRx (statistical), CU-DRx (statistical)
Bulusu et al. [12]	Single	Multiple	Yes	DTx-DRx (instantaneous), CU-DRx (1-bit feedback)
Yang et al. [13]	Single	Multiple	Yes	DTx-DRx (statistical), CU-DRx (statistical)
Ramezani-Kebrya et al. [14]	Single	Single	Yes	DTx-DRx (statistical), CU-DRx (statistical)
Li et al. [15]	Single	Multiple	No	DTx-DRx (statistical), CU-DRx (statistical)
Wang et al. [16]	Multiple	Multiple	No	DTx-DRx (instantaneous), CU-DRx (statistical)
Verenzuela et al. [17]	Multiple	Single	Yes	DTx-DRx (statistical), CU-DRx (statistical)
Gorantla et al. [18]	Multiple	Multiple	Yes	D2D SINR (quantized feedback)
Doumiati et al. [19]	Multiple	Multiple	No	DTx-DRx (statistical)
Xu et al. [21]	Multiple	Single	Yes	DTx-DRx (imperfect), CU-DRx (imperfect)
Hao et al. [22]	Multiple	Multiple	Yes	DTx-DRx (imperfect), CU-DRx (imperfect)

algorithms in [14]–[17], [20]–[22], RPA and CCSAA combine practically reasonable levels of CSI knowledge and signaling overhead with a performance guarantee on the D2D sum rate, while also controlling the implementation complexity. Lastly, SRU, which significantly improves the D2D sum rate, is novel compared to the literature.

There are several significant differences between our paper and [18]. First, only the partial CSI model is considered in [18], while we consider both partial and statistical CSI models and provide a unified algorithmic approach for them. Second, RPA is novel compared to [18] and provides a stronger performance guarantee. Third, while CCSAA was proposed in [18], it was only for the partial CSI model. Its applicability to the statistical CSI model is a contribution of this paper. Fourth, SRU outperforms the rate upgradation approach in [18].

#### D. Outline

The paper is organized as follows. Section II discusses the system model. Section III presents RPA, CCSAA, and SRU. Section IV presents performance benchmarking and numerical results. Our conclusions follow in Section V.

## II. SYSTEM MODEL

We consider  $N$  subchannels and  $M$  D2D pairs in a cell. Let  $\mathcal{D} = \{1, 2, \dots, M\}$  be the set of D2D pairs and  $\mathcal{S} = \{1, 2, \dots, N\}$  be the set of orthogonal uplink subchannels. The D2D pairs operate in the underlay mode and share subchannels with the CUs. We focus on the uplink subchannels for D2D assignment as this is preferred in 3GPP [26]. The CUs are already allocated to subchannels by the BS. Without loss of generality, let CU  $i$  be allocated to subchannel  $i$ . Therefore, the set of CUs is also  $\mathcal{S}$ .

The uplink channel power gain from CU  $i$  to the BS on subchannel  $i$  is  $h_{bi}(i)$ . The channel power gain from CU  $i$  to the DRx of D2D pair  $j$  on subchannel  $i$  is  $g_{ji}(i)$ . The channel power gain between the DTx and the DRx of D2D pair  $j$  on subchannel  $i$  is  $h_{jj}(i)$ , and from the DTx of D2D pair  $j$  to the BS is  $g_{jk}(i)$ . The channel power gain from the DTx of D2D

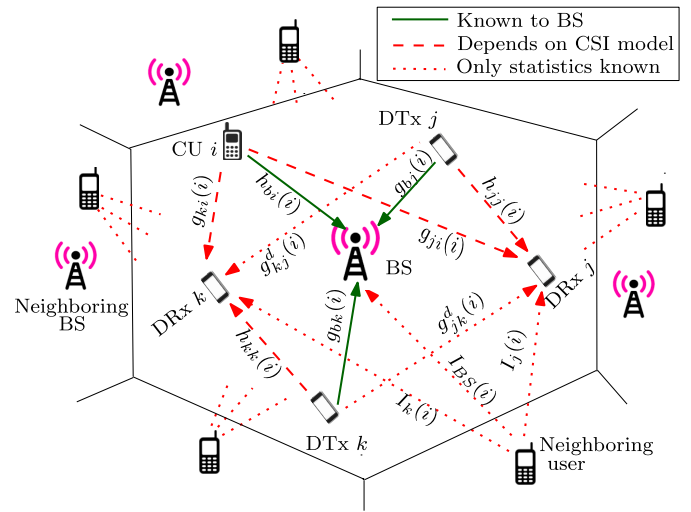


Fig. 1. System model depicting the various channels between the CU, D2D pairs, and BS. CSI of CU-to-BS and DTx-to-BS links is available at the BS, and the inter-cell interferences are unknown to the BS and DRxs. The CSI available at the DRx about the DTx-to-DRx and CU-to-DRx links depends on the CSI model.

pair  $k$  to the DRx of D2D pair  $j$  on subchannel  $i$  is  $g_{jk}^d(i)$ . Let  $L_{jj}$  be the path-loss of DTx-to-DRx link of D2D pair  $j$  and  $S_{jj}$  be its shadowing. Thus,  $h_{jj}(i)$  is the product of  $L_{jj}$ ,  $S_{jj}$ , and its small-scale fading power gain. Similarly,  $L_{bi}$  is the path-loss and  $S_{bi}$  is the shadowing of the link between CU  $i$  and the BS, and  $h_{bi}(i)$  is a product of  $L_{bi}$ ,  $S_{bi}$ , and its small-scale fading power gain. The system model is shown in Fig. 1.

**Fractional Power Control (FPC):** The CSI available at the BS fundamentally affects how the transmit power is controlled. For example, in the full CSI models of [4]–[8], the transmit power of the DTx of D2D pair  $j$  is a function of  $h_{jj}(i)$ ,  $g_{ji}(i)$ , and  $g_{jk}^d(i)$  since they are assumed to be known to the BS. However, this cannot be done in limited CSI models. We, therefore, use FPC, which is employed in 4G and 5G standards [27, Ch. 15]. To reduce the interference to other users, FPC only partially compensates for the path-loss and shadowing. In it, the transmit power  $P_j$  of the DTx of D2D

pair  $j$  is given by  $P_j = \min\{(\kappa_d\sigma^2)/(L_{jj}S_{jj})^\alpha, P_{\max}\}$ , where  $P_{\max}$  is the peak transmit power for the DTx,  $\kappa_d$  is a system parameter,  $\sigma^2$  is the noise variance, and  $0 \leq \alpha \leq 1$  is the fraction by which the path-loss and shadowing are compensated. Here,  $\alpha = 1$  implies complete compensation of the path-loss and shadowing while  $\alpha = 0$  implies no power control. Reducing  $\alpha$  causes less interference to other co-channel users. Similarly, the transmit power  $Q_i$  of CU  $i$  is given by  $Q_i = \min\{(\kappa_c\sigma^2)/(L_{bi}S_{bi})^\alpha, Q_{\max}\}$ , where  $Q_{\max}$  is the peak transmit power for the CU and  $\kappa_c$  is a system parameter. Note that the transmit power does not depend on the instantaneous interference.

*SINR of D2D Pair:* Let  $x_{ik}$  be an assignment variable that is 1 if D2D pair  $k$  is assigned to subchannel  $i$ , and is 0 otherwise. The SINR  $\zeta_j(i)$  of D2D pair  $j$  on subchannel  $i$  is given by

$$\zeta_j(i) = \frac{P_j h_{jj}(i)}{Q_i g_{ji}(i) + I_j^d(i) + \sigma^2}, \quad (1)$$

where  $I_j^d(i)$  is the sum of inter-cell interference and inter-D2D interference powers:

$$I_j^d(i) = \sum_{k=1, k \neq j}^M x_{ik} I_{jk}(i) + Z_j(i). \quad (2)$$

Here,  $Z_j(i)$  is the inter-cell interference power from the neighboring-cell users to the DRx of D2D pair  $j$  on subchannel  $i$  and  $I_{jk}(i)$  is the inter-D2D interference power from the DTx of D2D pair  $k$  to the DRx of D2D pair  $j$  on subchannel  $i$ .

#### A. Inter-D2D Interference and Inter-Cell Interference Model

The inter-D2D interference power  $I_{jk}(i)$  is given by  $I_{jk}(i) = P_k g_{jk}^d(i)$ . The instantaneous channel power gain  $g_{jk}^d(i)$ ,  $\forall j \neq k$ , is not known to the DRx of D2D pair  $j$  as it requires cooperation between the D2D pairs. Thus, the DRx of D2D pair  $j$  knows only the cumulative distribution function (CDF) of  $I_{jk}(i)$ ,  $\forall k \in \mathcal{S}, k \neq j$ . It can estimate the CDF of  $I_{jk}(i)$  by applying either parametric [28, Ch. 4] or non-parametric techniques [29] to its measurements of the interference from the DTx of D2D pair  $k$ .

The inter-cell interference power  $Z_j(i)$  is also not known to the DRx because it requires the DRx to know a priori which users will be scheduled in the neighboring cells and also the channel gains from those users. Therefore, the DRx of D2D pair  $j$  knows only the statistics of  $Z_j(i)$ . Similarly,  $Z_{BS}(i)$  is the inter-cell interference power from the neighboring-cell users to the BS. Only its statistics are known to the BS. As above, these statistics are obtained by the BS and the DRx by measuring the inter-cell interference over a period of time.

#### B. CSI Models

We consider the following two CSI models. In both models, the BS knows the instantaneous values of  $h_{bi}(i)$  and  $g_{bj}(i)$  as it is the receiver in those links. It can estimate them using the reference signals transmitted by CU  $i$  and D2D pair  $j$ .

*1) Partial CSI Model:* In this model, the DRx of D2D pair  $j$  knows the instantaneous values of  $h_{jj}(i)$  and  $g_{ji}(i)$ . Since the DRx does not know the inter-cell and inter-D2D interferences, it cannot know its SINR  $\zeta_j(i)$  on subchannel  $i$ . Despite this uncertainty, it can still compute an *SINR estimate*  $T_{ij}(\epsilon_d)$  such that when it transmits with the rate  $\log_2(1 + T_{ij}(\epsilon_d))$  bps/Hz, its outage probability is  $\epsilon_d$ . This is equivalent to

$$\Pr\left(\frac{P_j h_{jj}(i)}{Q_i g_{ji}(i) + I_j^d(i) + \sigma^2} \geq T_{ij}(\epsilon_d)\right) = 1 - \epsilon_d, \quad (3)$$

where  $\Pr(A)$  denotes the probability of an event  $A$ . Rearranging in terms of the CDF  $F_j(\cdot)$  of  $I_j^d(i)$ , we get

$$F_j\left(\frac{P_j h_{jj}(i)}{T_{ij}(\epsilon_d)} - Q_i g_{ji}(i) - \sigma^2\right) = 1 - \epsilon_d. \quad (4)$$

Rearranging terms again, we get

$$T_{ij}(\epsilon_d) = \frac{P_j h_{jj}(i)}{Q_i g_{ji}(i) + F_j^{-1}(1 - \epsilon_d) + \sigma^2}, \quad (5)$$

where  $F_j^{-1}(\cdot)$  is the inverse CDF of  $I_j^d(i)$ .

*Remark:* This formulation is general and applies to any statistical model of the inter-D2D and inter-cell interferences. Here,  $I_1^d(i), \dots, I_M^d(i)$  can be statistically non-identical and can be D2D pair-specific. For example, with Rayleigh fading and lognormal shadowing,  $I_j^d(i)$  can be accurately approximated as a lognormal random variable (RV) as it is the sum of composite Rayleigh-lognormal (Suzuki) RVs [30, Ch. 3]. Let the dB-mean and dB-standard deviation of  $I_j^d(i)$  be  $\mu_j$  and  $\sigma_j$ , respectively. Then, its inverse CDF  $F_j^{-1}(\cdot)$  can be shown to be  $F_j^{-1}(x) = 10^{0.1(\mu_j + \sigma_j Q^{-1}(1-x))}$ , for  $x \geq 0$ , where  $Q^{-1}(\cdot)$  is the inverse Q-function. In practice, the CDF  $F_j(\cdot)$  can be estimated by the DRx from its measurements of  $I_j^d(i)$  using techniques mentioned in Section II-A. The above formulation can also incorporate imperfect CSI. For example, let  $\hat{H}_{jj}(i)$  be the imperfect estimate for the complex channel gain  $H_{jj}(i)$  of the DTx-DRx link of D2D pair  $j$  on subchannel  $i$ . This changes (3) to

$$\Pr\left(\frac{P_j |H_{jj}(i)|^2}{Q_i g_{ji}(i) + I_j^d(i) + \sigma^2} \geq T_{ij}(\epsilon_d) | \hat{H}_{jj}(i)\right) = 1 - \epsilon_d.$$

Rearranging terms yields the expression for  $T_{ij}(\epsilon_d)$  in terms of the conditional CDF of  $H_{jj}(i)$  given  $\hat{H}_{jj}(i)$ . The conditional CDF depends on the estimator used.

*2) Statistical CSI Model:* In this model, the DRx of D2D pair  $j$  knows only the statistics of  $h_{jj}(i)$  and  $g_{ji}(i)$ . This is practically easier since the statistics change at a much slower timescale. As in the partial CSI model, the DRx faces several uncertainties in knowing its SINR. However, using the statistical information, it can still compute an SINR estimate  $T_{ij}(\epsilon_d)$  such that the rate  $\log_2(1 + T_{ij}(\epsilon_d))$  is in outage with probability  $\epsilon_d$ . The calculations are as follows.

In the SINR expression in (1), the numerator is a Suzuki RV. It can be accurately approximated as a lognormal RV with dB-mean  $\mu'_j$  and dB-variance  $\sigma'^2_j$  [30, (2.188)]. Similarly, the denominator is a sum of Suzuki RVs and a constant. Hence, it can also be accurately approximated as a lognormal RV with dB-mean  $\mu''_{ij}$  and dB-variance  $\sigma''^2_{ij}$ , which are found

using the Fenton-Wilkinson method [30, Ch. 3]. Note that  $\mu''_{ij}$  and  $\sigma''_{ij}$  depend on  $i$  because the statistics of the CU-to-DRx interference depends on  $i$ .

Thus, the SINR  $\zeta_j(i)$  can be approximated as a ratio of two lognormal RVs, which again is a lognormal RV with dB-mean  $\tilde{\mu}_{ij} = \mu'_j - \mu''_{ij}$  and dB-variance  $\tilde{\sigma}_{ij}^2 = \sigma_j'^2 + \sigma_{ij}''^2$ . Therefore, as above, we compute  $T_{ij}(\epsilon_d)$  such that the SINR  $\zeta_j(i)$  lies below it with probability  $\epsilon_d$ :

$$\Pr(\zeta_j(i) < T_{ij}(\epsilon_d)) = \epsilon_d. \quad (6)$$

Using the expression for the CDF of a lognormal RV, and simplifying, we get

$$T_{ij}(\epsilon_d) = 10^{0.1(\tilde{\mu}_{ij} + \tilde{\sigma}_{ij} Q^{-1}(1 - \epsilon_d))}. \quad (7)$$

### C. Quantization and Feedback

Let  $0 = \Psi_0 < \Psi_1 < \dots < \Psi_{L-1} < \infty$  be the  $L = 2^q$  quantization thresholds. These are pre-specified and are known to the DTxs, DRxs, and BS. The D2D pair  $j$  quantizes  $T_{ij}(\epsilon_d)$  to one among the  $L$  quantization thresholds and feeds it back to the BS using a  $q$ -bit feedback  $\delta_{ij}$  as follows:

$$\delta_{ij} = l, \text{ if } \Psi_l \leq T_{ij}(\epsilon_d) < \Psi_{l+1}. \quad (8)$$

Given  $\delta_{ij}$ , the BS determines the rate  $C_{ij}$  of the D2D pair  $j$  on subchannel  $i$  as

$$C_{ij} = \log_2(1 + \Psi_{\delta_{ij}}). \quad (9)$$

Since the rate depends logarithmically on the SINR, quantizing the SINR in dB scale is equivalent to quantizing the rate.

The only information the BS has about the rate of the D2D pair  $j$  is  $C_{ij}$ . It is less than or equal to  $\log_2(1 + T_{ij}(\epsilon_d))$  due to the quantization in (8). This again ensures that  $C_{ij}$  is in outage with probability at most  $\epsilon_d$ .

### D. D2D Assignment Limit to Control Inter-D2D Interference

Assigning multiple D2D pairs to a subchannel can improve spatial reuse. However, it also increases the inter-D2D interference between them, which can decrease their rates. To control the inter-D2D interference and investigate the potential trade-off between it and the spatial reuse gain, we allow at most  $K$  D2D pairs to share a subchannel. We shall refer to  $K$  as the *D2D assignment limit*. Therefore,  $\sum_{j=1}^M x_{ij} \leq K$ .

Note that the total inter-D2D interference power  $\sum_{k=1, k \neq j}^M x_{ik} I_{jk}(i)$  in (2) is not known to the DRx when it generates feedback because it does not yet know which other D2D pairs will share a subchannel with it. Limiting the number of D2D pairs that can share a subchannel to  $K$  enables us to compute a conservative estimate of the inter-D2D interference that provides a reliability guarantee to the D2D users. We achieve this by considering the interference from the  $K - 1$  D2D pairs closest to the DRx of D2D pair  $j$  to determine the CDF of  $I_j^d(i)$  in (2). Therefore, we replace  $\sum_{k=1, k \neq j}^M x_{ik} I_{jk}(i)$  in (2) with  $\sum_{k=1}^{K-1} I_{j(k)}(i)$ , where  $(k)$  denotes the  $k^{\text{th}}$  closest DTx from the DRx of D2D pair  $j$ , and use its statistics instead in (5) and (7). As a consequence of this, both  $T_{ij}(\epsilon_d)$  and  $C_{ij}$  are now functions of  $K$ , and they decrease as  $K$  increases.

### E. QoS Guarantee for CUs

The SINR  $\xi_i$  of CU  $i$  on its allocated subchannel  $i$  is

$$\xi_i = \frac{Q_i h_{bi}(i)}{\sum_{j=1}^M x_{ij} P_j g_{bj}(i) + Z_{BS}(i) + \sigma^2}. \quad (10)$$

The BS receiver experiences inter-cell interference and interference from the D2D pairs that share the subchannel with CU  $i$ . We require that CU  $i$  must be able to transmit at a minimum rate  $R_{\min}^{(i)}$  bps/Hz with a probability of outage at most  $\epsilon_c$ , where  $R_{\min}^{(i)}$  and  $\epsilon_c$  are system parameters:

$$\Pr(\log_2(1 + \xi_i) \geq R_{\min}^{(i)}) \geq 1 - \epsilon_c. \quad (11)$$

Substituting the SINR  $\xi_i$  expression from (10) and rearranging terms, we get

$$\sum_{j=1}^M x_{ij} w_{ij} \leq b_i, \quad (12)$$

where  $w_{ij} = P_j g_{bj}(i)$  is the interference power at the BS on subchannel  $i$  due to the DTx of D2D pair  $j$ ,  $b_i = Q_i h_{bi}(i) / (2^{R_{\min}^{(i)}} - 1) - \sigma^2 - F_{BS}^{-1}(1 - \epsilon_c)$ , and  $F_{BS}^{-1}(\cdot)$  is the inverse CDF of  $Z_{BS}(i)$ . As in Section II-B,  $Z_{BS}(i)$  can be approximated as a lognormal RV with dB-mean  $\mu_B$  and dB-standard deviation  $\sigma_B$ . Then,  $F_{BS}^{-1}(x) = 10^{0.1(\mu_B + \sigma_B Q^{-1}(1-x))}$ , for  $x \geq 0$ . Note that  $b_i$  depends on  $h_{bi}(i)$  and the parameters  $R_{\min}^{(i)}$  and  $\epsilon_c$ .

## III. UNIFIED SUBCHANNEL ALLOCATION PROBLEM AND POLYNOMIAL-TIME ALGORITHMS

For both CSI models, the problem of allocating multiple D2D pairs to subchannels to maximize the sum of D2D rates can be stated mathematically as follows:

$$\mathcal{P} : \max_{x_{ij}, \forall i \in \mathcal{S}, j \in \mathcal{D}} \left\{ \sum_{i=1}^N \sum_{j=1}^M x_{ij} C_{ij} \right\}, \quad (13)$$

$$\text{subject to } \sum_{i=1}^N x_{ij} \leq 1, \quad \forall j \in \mathcal{D}, \quad (14)$$

$$\sum_{j=1}^M x_{ij} w_{ij} \leq b_i, \quad \forall i \in \mathcal{S}, \quad (15)$$

$$\sum_{j=1}^M x_{ij} \leq K, \quad \forall i \in \mathcal{S}, \quad (16)$$

$$x_{ij} \in \{0, 1\}, \quad \forall i \in \mathcal{S}, j \in \mathcal{D}. \quad (17)$$

Note that  $C_{ij}$  in the objective function depends on the CSI model and  $K$ . The transmit power set by FPC influences  $\mathcal{P}$  in multiple ways. First, it influences the objective function in (13) since  $C_{ij}$  is a function of the SINR estimate  $T_{ij}(\epsilon_d)$ , which depends on both D2D and CU transmit powers. It also influences the constraint in (15) since  $w_{ij}$  and  $b_i$  depend on the D2D transmit power and CU transmit power, respectively.

In  $\mathcal{P}$ , constraint (14) mandates that at most one subchannel can be assigned to a D2D pair, (15) specifies a minimum rate guarantee for the CUs, and (16) ensures that at most  $K$  D2D pairs are assigned to a subchannel.  $\mathcal{P}$  is a binary integer

programming problem that is NP-hard [23]. We present two algorithms to solve  $\mathcal{P}$ . They are based on different approaches and provide different performance guarantees.<sup>1</sup>

### A. Relaxation-Pruning Algorithm (RPA)

RPA consists of four steps. First, we solve an integer-relaxed version of  $\mathcal{P}$ . Second, using this solution, we construct a bipartite graph between the D2D pairs and the subchannels. Third, we determine the maximum weighted matching for the bipartite graph. This leads to an allocation of the D2D pairs to subchannels. However, it can violate the constraint in (15). In such a case, the matching is pruned to arrive at a feasible integer solution in the fourth step. The steps are described in detail below. The rationale behind them will come out in the proof of the performance guarantee in Result 1.

1) For all  $i \in \mathcal{S}$ ,  $j \in \mathcal{D}$ , we set  $x_{ij} = 0$  if  $w_{ij} > b_i$ , since the D2D pair  $j$  will violate (15) and can never be assigned to subchannel  $i$ . For all other  $x_{ij}$ , the binary integer constraint in (17) is relaxed to  $0 \leq x_{ij} \leq 1$ . This changes  $\mathcal{P}$  to a linear program, which is optimally solved in polynomial time by using the dual simplex [31, Ch. 4] or interior-point methods [31, Ch. 5]. Let  $\tilde{x}_{ij}$ ,  $\forall i \in \mathcal{S}, j \in \mathcal{D}$ , be the optimal solution to the linear program. We shall refer to  $\tilde{x}_{ij}, \forall j \in \mathcal{D}$ , as the *fractional solution* for subchannel  $i$ .

2) For each subchannel  $i$ , compute  $n_i = \lceil \sum_{j=1}^M \tilde{x}_{ij} \rceil$ , where  $\lceil \cdot \rceil$  denotes the ceiling function. Clearly,  $n_i \leq K$  since (16) implies that  $\sum_{j=1}^M \tilde{x}_{ij} \leq K$ . We construct a bipartite graph with  $\sum_{i=1}^N n_i$  vertices on one side and  $M$  D2D pairs as vertices on the other side. For each subchannel  $i$ , the construction proceeds as follows:

- Create  $n_i$  copies of the subchannel  $i$ , which are denoted by  $i_1, i_2, \dots, i_{n_i}$ . Henceforth, we shall refer to these as *virtual subchannels* of  $i$ .
- Consider the set of D2D pairs  $\mathcal{D}'_i = \{j : \tilde{x}_{ij} \neq 0, j \in \mathcal{D}\}$ , whose fractional solution for subchannel  $i$  is non-zero. Arrange the D2D pairs in  $\mathcal{D}'_i$  in the non-increasing order of their interference power to the BS:

$$w_{i[1]} \geq w_{i[2]} \geq \dots \geq w_{i[|\mathcal{D}'_i|]}. \quad (18)$$

Here, using order statistics notation,  $[k]$  is the D2D pair in  $\mathcal{D}'_i$  that causes the  $k^{\text{th}}$  largest interference to the BS and  $|\mathcal{D}'_i|$  denotes the cardinality of  $\mathcal{D}'_i$ .

- Let  $j_1$  be such that  $\tilde{x}_{i[1]} + \tilde{x}_{i[2]} + \dots + \tilde{x}_{i[j_1-1]} < 1$  and  $\tilde{x}_{i[1]} + \dots + \tilde{x}_{i[j_1-1]} + \tilde{x}_{i[j_1]} \geq 1$ . Then, construct edges between virtual subchannel  $i_1$  and D2D pairs  $[1], [2], \dots, [j_1]$ .
- An edge between  $i_2$  and  $[j_1]$  is constructed only if  $\tilde{x}_{i[1]} + \dots + \tilde{x}_{i[j_1-1]} + \tilde{x}_{i[j_1]} > 1$ . Let  $j_2$  be such that  $\tilde{x}_{i[1]} + \dots + \tilde{x}_{i[j_1]} + \dots + \tilde{x}_{i[j_2-1]} < 2$  and  $\tilde{x}_{i[1]} + \dots + \tilde{x}_{i[j_1]} + \dots + \tilde{x}_{i[j_2-1]} + \tilde{x}_{i[j_2]} \geq 2$ . Construct edges between  $i_2$  and D2D pairs  $[j_1 + 1], [j_1 + 2], \dots, [j_2]$ .
- In general, let  $j_k$  be such that  $\sum_{j=1}^{j_k-1} \tilde{x}_{i[j]} < k$  and  $\sum_{j=1}^{j_k} \tilde{x}_{i[j]} \geq k$ , for  $k = 1, 2, \dots, n_i$ . Edges are constructed between virtual subchannel  $i_{k+1}$  and D2D pairs

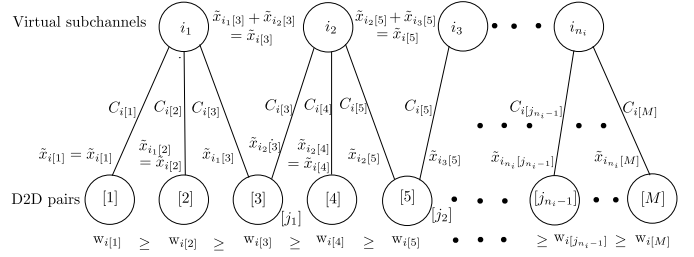


Fig. 2. Example showing the edges in the bipartite graph between the D2D pairs and the virtual subchannels for subchannel  $i$ .

$[j_k + 1], [j_k + 2], \dots, [j_{k+1}]$ . Also, an edge is constructed between  $i_{k+1}$  and  $[j_k]$  only if  $\sum_{j=1}^{j_k} \tilde{x}_{i[j]} > k$ .

- The weight of the edge formed between any virtual subchannel of  $i$  and D2D pair  $j$  is  $C_{ij}$ . The bipartite graph for subchannel  $i$  is shown in Fig. 2.

3) Run the Kuhn-Munkres algorithm [32, Ch. 3] to find the optimal maximum weighted matching for the above bipartite graph. It solves the following optimization problem  $\mathcal{Q}$ :

$$\mathcal{Q} : \max_{y_{ij}, \forall i, l, j} \sum_{i=1}^N \sum_{l=1}^{n_i} \sum_{j=1}^M y_{ij} C_{ij}, \quad (19)$$

$$\text{subject to } \sum_{i=1}^N \sum_{l=1}^{n_i} y_{ij} \leq 1, \quad \forall j \in \mathcal{D}, \quad (20)$$

$$\sum_{j=1}^M y_{ij} \leq 1, \quad \forall i \in \mathcal{S}, l \in \{1, \dots, n_i\}, \quad (21)$$

$$y_{ij} \in \{0, 1\}, \quad \forall i \in \mathcal{S}, l \in \{1, \dots, n_i\}, j \in \mathcal{D}, \quad (22)$$

where  $y_{ij}$  is the binary matching variable that is 1 if the edge between virtual subchannel  $i_l$  and D2D pair  $j$  is selected, and is 0 otherwise. Thus, the algorithm selects the edges in such a way that the sum of the weights of the selected edges is maximized. It ensures that at most one virtual subchannel is connected to a D2D pair, which is the constraint in (20), and at most one D2D pair is connected to a virtual subchannel, which is the constraint in (21). When an edge between any virtual subchannel of  $i$  and D2D pair  $j$  is selected by the algorithm, we say that D2D pair  $j$  is assigned to subchannel  $i$ . We shall refer to this assignment as the *integral matching solution*. It is possible that this assignment may not satisfy the constraint in (15) for some subchannels since  $\mathcal{Q}$  does not consider it.

4) Prune those parts of the integral matching solution that do not satisfy the constraint in (15). We refer to assignments of D2D pairs to subchannels that satisfy (15) as feasible assignments and the rest as infeasible assignments. Let subchannel  $i$  be a subchannel with an infeasible assignment that has virtual subchannels  $i_1, i_2, \dots, i_{n_i}$  assigned to the D2D pairs  $k_1, k_2, \dots, k_{n_i}$ , respectively.<sup>2</sup> Their interference powers to the BS are in the descending order:  $w_{ik_1} \geq w_{ik_2} \geq \dots \geq w_{ik_{n_i}}$ . If  $C_{ik_1} \geq C_{ik_2} + \dots + C_{ik_{n_i}}$ , then only D2D pair  $k_1$  is allocated

<sup>1</sup>The algorithms we propose below can also be applied to the full CSI model. This is done by setting  $C_{ij} = \log_2(1 + \zeta_j(i))$  in the objective function in (13).

<sup>2</sup>This description also includes the scenario where a virtual subchannel, say  $i_l$ , is not assigned to any D2D pair. In that case, the D2D pair  $k_l$  is not considered in the above assignment.

to subchannel  $i$ . Otherwise, the D2D pairs  $k_2, \dots, k_{n_i}$  are all allocated to subchannel  $i$ . As shown in Lemma 1 below, this assignment is feasible. This yields the final allocation of the D2D pairs to subchannels.

*Lemma 1:* Pruning in Step 4 yields a feasible assignment, i.e., the D2D pairs allocated to a subchannel satisfy the interference constraint in (15).

*Proof:* The proof is relegated to Appendix A. ■  
RPA provides the following theoretical performance guarantee.

*Result 1:* The D2D sum rate of RPA is at least half of the optimal D2D sum rate.

*Proof:* The proof is given in Appendix B. ■

1) *Computational Complexity:* The linear program in Step 1 has a complexity of  $\mathcal{O}(N^3M^3)$  [31, Ch. 5]. Step 2 has a complexity of  $\mathcal{O}(NM \log M)$ . The Kuhn-Munkres algorithm in Step 3 has a complexity of  $\mathcal{O}((N + 2M)^3)$  [32, Ch. 3]. The pruning step in Step 4 has a complexity of  $\mathcal{O}(NM \log M)$ . Combining these, the complexity of RPA is  $\mathcal{O}(N^3M^3)$ .

2) *Special Cases:* When  $K = 1$ , RPA arrives at the optimal solution of  $\mathcal{P}$ . This is because the D2D pair  $j$  whose  $w_{ij}$  exceeds  $b_i$  will be discarded for allocation to subchannel  $i$  in Step 1 itself. All the D2D pairs that are considered for allocation in Steps 2 and 3 satisfy (15). Therefore, Step 4 is never required in this case. Hence, the D2D sum rate achieved in Step 3 is optimal, as can be seen from Appendix B.

Another instance where RPA is optimal is when  $b_i, \forall i \in \mathcal{S}$ , are sufficiently large such that the constraint in (15) is always satisfied for all subchannels. This occurs when  $R_{\min}^{(i)}$  is small or  $Q_i$  is large,  $\forall i \in \mathcal{S}$ .

## B. CCSAA

CCSAA approaches  $\mathcal{P}$  as a submodular maximization problem. We refer the reader to [18] for a formal description of the algorithm. While CCSAA is proposed in [18], its applicability to the statistical CSI model is a contribution of this paper.

CCSAA uses two concepts, namely, *feasible set* and *incremental gain*. A feasible set for a subchannel is a set of D2D pairs that satisfies the constraints in (15) and (16). There can be several feasible sets for a subchannel. CCSAA first selects a feasible set  $\nu_1$  for subchannel 1. It then selects a feasible set  $\nu_2$  for subchannel 2, and so on. A D2D pair can belong to one or more of the selected feasible sets of the subchannels.

Selecting a feasible set for a subchannel is based on the incremental gain, which is defined as follows. For subchannel  $i$ , the incremental gain  $p_{ij}$  of D2D pair  $j$  is  $C_{ij}$  if the D2D pair is not present in the selected feasible sets of subchannels  $1, \dots, i-1$ . If it is present, then  $p_{ij}$  is the difference between  $C_{ij}$  and the maximum rate on those subchannels in which it belongs to their selected feasible sets. Hence,  $p_{ij} = \max \left\{ C_{ij} - \max_{l=1, \dots, i-1} \{C_{lj} : \exists j \in \nu_l\}, 0 \right\}$ . The incremental gain of a feasible set is defined as the sum of the incremental gains of the D2D pairs in it.

For a subchannel, the goal is to select a feasible set that has the maximum incremental gain. This turns out to be a cardinality-constrained knapsack problem (CCKP), which is NP-hard. Therefore, to select a feasible set, CCSAA uses the following approach [25]. First, a linear program, which

is formed by relaxing the binary assignment constraints of CCKP, is solved. The elements of the resulting solution are then deterministically rounded-off to 0 or 1. The rounding is done such that the resulting set is feasible and ensures that the incremental gain of that set is at least half of the incremental gain of an optimal feasible set.

Once the feasible sets are selected for all the subchannels, then the D2D pairs in the selected feasible set of a subchannel are all allocated to that subchannel. If a D2D pair is present in the selected feasible sets of more than one subchannel, then it is allocated to the subchannel for which it has the maximum rate. Akin to RPA, CCSAA also comes with the following desirable performance guarantee. Its proof is given in [18] and is not repeated here.

*Result 2:* The D2D sum rate of CCSAA is at least one-third of the optimal D2D sum rate.

*Computational Complexity:* Finding the feasible D2D set for a subchannel involves solving a linear program in  $M$  variables. It has a complexity of  $\mathcal{O}(M^2 \log M)$  [33]. Since this is done for  $N$  subchannels, the complexity of CCSAA is  $\mathcal{O}(NM^2 \log M)$ .

## C. Contrasting Aspects of RPA and CCSAA

CCSAA approaches  $\mathcal{P}$  as a submodular maximization problem as opposed to the linear program relaxation and rounding approach that RPA employs. In CCSAA, the D2D pairs are allocated sequentially, i.e., the D2D pairs are first allocated to subchannel 1, then subchannel 2, and so on. On the other hand, all the subchannels are considered simultaneously for allocating D2D pairs in RPA. In CCSAA, a D2D pair can belong to feasible sets of multiple subchannels, and is allocated to the subchannel with the maximum rate. However, in RPA, a D2D pair is never assigned to more than one subchannel in any step. RPA has a better performance guarantee than CCSAA, while CCSAA has a lower computational complexity than RPA. As we shall see, the different design approaches of the algorithms lead to different responses for the two CSI models in Section IV.

## D. Statistical Rate Upgradation (SRU)

In calculating the rate  $C_{ij}$  or equivalently  $T_{ij}(\epsilon_d)$ , the DRx considered the interference from the  $K-1$  closest D2D pairs. Once the BS assigns the D2D pairs to subchannels, the assignment information can be exploited by the D2D pair to improve its rate as follows.<sup>3</sup>

Given  $x_{ik}, \forall k \in \mathcal{D}$ , the DRx can compute the exact statistics of  $\sum_{k=1, k \neq j}^M x_{ik} I_{jk}(i)$  in (2) instead of  $\sum_{k=1}^{K-1} I_{j(k)}(i)$ . Therefore, the DRx uses  $I_j^d(i) = \sum_{k=1, k \neq j}^M x_{ik} I_{jk}(i) + Z_j(i)$  in both CSI models to compute a new SINR threshold  $T_{ij}'(\epsilon_d) \geq T_{ij}(\epsilon_d)$ . The DRx communicates this to the DTx, which increases its rate from  $C_{ij}$  to  $\log_2(1 + T_{ij}'(\epsilon_d))$ . We refer to this process as SRU. The outage probability of the rate after SRU is still at most  $\epsilon_d$  for any D2D pair.

<sup>3</sup>This is practically implementable when the BS broadcasts the allocation information after running the allocation algorithm.

TABLE II  
 QUANTIZATION THRESHOLDS IN dB

$q$	Partial CSI Model	Statistical CSI Model
1	$\Psi_1 = 8$	$\Psi_1 = -2$
2	$\Psi_1 = 4, \Psi_2 = 8, \Psi_3 = 12$	$\Psi_1 = -4, \Psi_2 = -2, \Psi_3 = 0$
4	$\Psi_1 = 1, \Psi_2 = 2, \Psi_3 = 3, \Psi_4 = 4, \Psi_5 = 5, \Psi_6 = 6, \Psi_7 = 7, \Psi_8 = 8, \Psi_9 = 9, \Psi_{10} = 10, \Psi_{11} = 11, \Psi_{12} = 12, \Psi_{13} = 13, \Psi_{14} = 14, \Psi_{15} = 15$	$\Psi_1 = -10, \Psi_2 = -8, \Psi_3 = -6, \Psi_4 = -4, \Psi_5 = -2, \Psi_6 = 0, \Psi_7 = 2, \Psi_8 = 4, \Psi_9 = 6, \Psi_{10} = 8, \Psi_{11} = 10, \Psi_{12} = 12, \Psi_{13} = 14, \Psi_{14} = 16, \Psi_{15} = 18$

#### IV. NUMERICAL RESULTS AND PERFORMANCE BENCHMARKING

We now present Monte Carlo simulation results for the following setting. The  $N$  CUs and the DRxs of the  $M$  D2D pairs are dropped with uniform probability within a cell of radius 500 m. The DTx lies with uniform probability within a circle of radius 50 m around the DRx. This models the different DTx-DRx distances in different D2D pairs. As specified in 3GPP [34], the path-loss in dB for the DTx-to-DRx and CU-to-DRx links is  $148 + 40 \log_{10}(d)$ , and for the CU-to-BS and DTx-to-BS links is  $128.1 + 37.6 \log_{10}(d)$ , where  $d$  is the distance in km. We illustrate the results for Rayleigh fading, lognormal shadowing with a dB-standard deviation of 6,  $\sigma^2 = -114$  dBm,  $\epsilon_c = 0.1$ , and  $R_{\min}^{(i)} = 1$  bps/Hz,  $\forall i \in \mathcal{S}$ . The FPC parameters are  $\alpha = 0.8$ ,  $\kappa_c = 25$  dB,  $\kappa_d = 30$  dB,  $P_{\max} = 21$  dBm, and  $Q_{\max} = 24$  dBm [4], [10]. The simulation results are averaged over 10000 user drops and channel realizations.

The SINR quantization thresholds for the two CSI models are enumerated in Table II. For the partial CSI model, they are centered around 8 dB; they span a 8 dB range for  $q = 2$  bits and a 14 dB range for  $q = 4$  bits. In the statistical CSI model, the SINR estimate  $T_{ij}(\epsilon_d)$  is smaller. Therefore, the thresholds are centered around  $-2$  dB, and they span a 4 dB range for  $q = 2$  bits and a 28 dB range for  $q = 4$  bits.

*Inter-cell Interference Statistics:* Since the scheduler in one cell is independent of those in the other cells, the statistics of the inter-cell interference, which the DRx uses to compute  $T_{ij}(\epsilon_d)$ , are obtained as follows. For a subchannel, one CU and  $\min\{K, \lceil M/N \rceil\}$  D2D pairs are dropped with uniform probability in each of the neighboring cells. Here,  $M/N$  is the average number of D2D pairs per subchannel. The small-scale fading and lognormal shadowing are generated for the links from these neighboring cell users to the BS and the DRxs. The interferences seen at the BS and the DRxs are measured. The empirical CDFs of  $Z_j(i)$ ,  $\forall j \in \mathcal{D}$ , and  $Z_{BS}(i)$  are determined from 10000 such measurements. The sum of  $\sum_{k=1, k \neq j}^M x_{ik} I_{jk}(i)$  and  $Z_j(i)$  in (2) is approximated as a lognormal RV using the Fenton-Wilkinson method [30, Ch. 3].

##### A. Benchmarking Schemes

We compare the D2D sum throughputs of RPA and CCSAA with the following schemes. For a D2D pair, the throughput is equal to its assigned rate if the transmission is not in outage, which happens when the instantaneous SINR is greater than

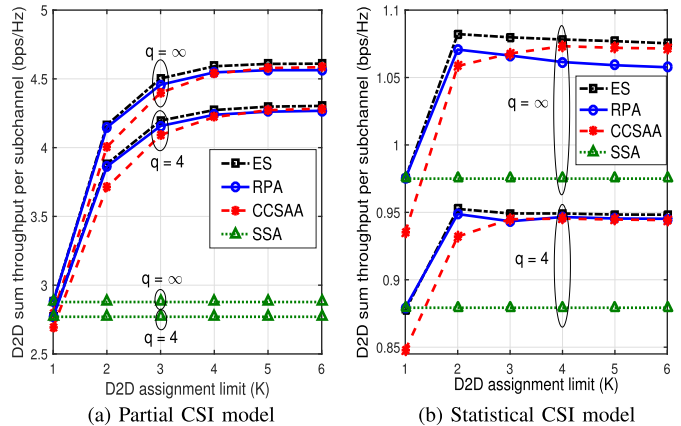


Fig. 3. Benchmarking: Zoomed-in comparison of the sum throughputs per subchannel of RPA and CCSAA with ES and SSA for small user counts ( $N = 4$ ,  $M = 6$ , and  $\epsilon_d = 0.1$ ).

or equal to  $\Psi_{\delta_{ij}}$ , otherwise it is zero. We focus on throughput because it accounts for outages.

- *Exhaustive Search (ES):* In this, the optimal solution of  $\mathcal{P}$  is found by searching over all possible assignments of D2D pairs to subchannels. Therefore, ES serves as an upper bound for any algorithm. Since the number of possible assignments is  $2^{MN}$ , ES is computationally infeasible except for small values of  $N$  and  $M$ .
- *Semi-orthogonal Sharing Assignment (SSA)* [4], [5], [10], [11], [15]: In this, at most one D2D pair can be assigned to a subchannel. SSA completely avoids inter-D2D interference. The optimal subchannel allocation is found using the Kuhn-Munkres algorithm.

A comparison with the approaches in [6]–[8], [16], [17], [20]–[22] that also consider multiple D2D pairs per subchannel is not possible due to fundamental differences in the CSI model, QoS guarantees, number of subchannels available, and the objective function. For example, the BS is assumed to have full CSI in [6]–[8]. As a result, the allocation and power control algorithms designed for it cannot be applied to the limited CSI models that we consider. Only one subchannel is considered in [17], [20], [21], while we consider multiple subchannels. This makes the problem formulation different because a D2D pair can now be potentially assigned to any of the subchannels. QoS guarantees are not provided in [7], while those in [16], [17], [22] are different from ours and so are the objective functions.

##### B. Numerical Results

Fig. 3 benchmarks the performance of RPA and CCSAA with ES and SSA. Given the exponential complexity of ES, this is done for small values of  $M$  and  $N$ . Fig. 3a plots the D2D sum throughput per subchannel as a function of the D2D assignment limit  $K$  for the partial CSI model. The sum throughput of RPA is indistinguishable from that of ES for  $K \leq 2$ , and is within 1% for  $K \geq 3$ . It is higher than that of CCSAA for  $K \leq 3$ . The sum throughputs of the two algorithms are close to each other and to that of ES for  $K \geq 4$ . This validates the lower bounds on the performance

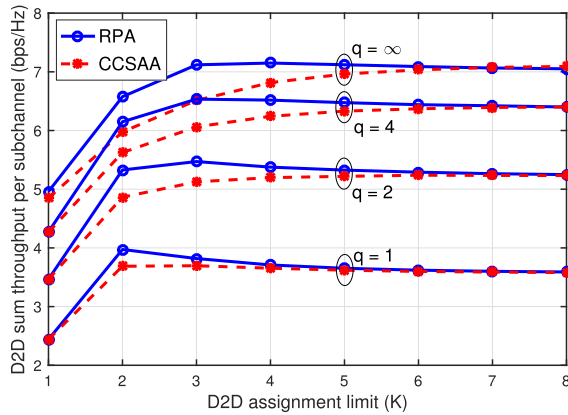


Fig. 4. Partial CSI model: Comparison of the sum throughputs per subchannel of RPA and CCSAA for different  $K$  and  $q$  ( $N = 10$ ,  $M = 30$ , and  $\epsilon_d = 0.1$ ).

of RPA and CCSAA, which are not shown to avoid clutter. Since SSA is not a function of  $K$ , it is a horizontal line. RPA and CCSAA significantly outperform SSA because they can assign multiple D2D pairs to a subchannel and can effectively deal with the resultant inter-D2D interference. As  $K$  increases, the sum throughput increases because more D2D pairs are allowed to share the same subchannel, which improves spatial reuse.

Fig. 3b plots the corresponding results for the statistical CSI model. For  $q = \infty$ , the sum throughput of CCSAA increases as  $K$  increases and is within 1% of that of ES at  $K = 6$ . The maximum sum throughput of RPA, which occurs at  $K = 2$ , is within 1% of that of ES. Similarly, for  $q = 4$ , the sum throughput of CCSAA at  $K = 6$  is within 1% of ES, and that of RPA at  $K = 2$  is within 0.5% of ES. As above, this also validates the lower bounds of RPA and CCSAA for the statistical CSI model. For  $K \geq 2$ , CCSAA performs better than RPA. We now delve deeper into the behavior of RPA and CCSAA for larger values of  $M$  and  $N$ . Therefore, we can no longer show results for ES.

Fig. 4 plots the sum throughputs per subchannel of RPA and CCSAA as a function of  $K$  for the partial CSI model for  $q = 1, 2, 4$ , and  $\infty$ . As  $K$  increases, the sum throughput of RPA increases and then decreases. The decrease is visible for  $q = 1$  and 2, but is imperceptible for  $q \geq 4$ . As above, the increase occurs because more D2D pairs are allowed to share the same subchannel. For  $K \geq 3$ , the decrease occurs because the inter-D2D interference, which is set as  $\sum_{k=1}^{K-1} I_j^{(k)}(i)$  to determine  $T_{ij}(\epsilon_d)$  (cf. Section II-D), increases. This decreases the rate  $C_{ij}$ .

The trends are different for CCSAA. Now, the sum throughput monotonically increases as  $K$  increases for  $q \geq 2$  and eventually saturates. The saturation occurs because the average number of D2D pairs per subchannel is  $M/N$ . Thus, making  $K$  large effectively removes any limit on the number of D2D pairs that can be assigned the same subchannel. Only for  $q = 1$  is the trend similar to RPA. Here, the optimal value of  $K$  that maximizes the sum throughput is 2. For both algorithms, as  $q$  increases, the sum throughput increases because the higher feedback resolution leads to a higher rate (cf. (9)). RPA

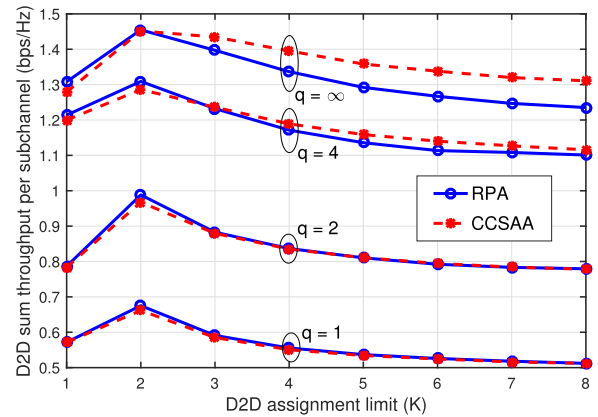


Fig. 5. Statistical CSI model: Comparison of the sum throughputs per subchannel of RPA and CCSAA for different  $K$  and  $q$  ( $N = 10$ ,  $M = 30$ , and  $\epsilon_d = 0.1$ ).

outperforms CCSAA for small  $K$ , while the two algorithms are indistinguishable for  $K \geq 6$ . For  $K = 1$ , since RPA is provably optimal, its sum throughput is always greater than or equal to that of CCSAA.

Fig. 5 plots the corresponding results for the statistical CSI model. Here, the sum throughputs of both algorithms are lower and are more sensitive to  $K$ . As  $K$  increases, their sum throughputs increase up to  $K = 2$  and then decrease. The decrease occurs because of the increase in the inter-D2D interference as  $K$  increases. Thus, inter-D2D interference has a more pronounced impact in the statistical CSI model. Another noteworthy difference compared to the partial CSI model is that CCSAA outperforms RPA for  $K \geq 3$ , despite its weaker performance guarantee. We observe that the maximum sum throughputs for RPA and CCSAA are achieved at  $K = 2$  for all  $q$ , which is different from what we observed for the partial CSI model. As before, as  $q$  increases, the sum throughput increases due to more feedback.

#### Interplay Between CSI Models and Algorithms:

Figs. 4 and 5 bring out a noticeable difference in the behavior of the two algorithms for the two CSI models. The sum throughput for the partial CSI model is higher than that for the statistical CSI model because the DRx knows the instantaneous channel gains of the DTx-to-DRx and CU-to-DRx links instead of just their statistics. RPA performs better than CCSAA for the partial CSI model, while the reverse is true for the statistical CSI model. In the statistical CSI model, the channel statistics of the CU-to-DRx links vary much less from one subchannel to another than the instantaneous channel gains of the DTx-to-DRx and CU-to-DRx links in the partial CSI model. As a result, the variation in the rate  $C_{ij}$  is much more from one subchannel to another in the partial CSI model than in the statistical CSI model. The contrasting designs of RPA and CCSAA react to this variation differently. RPA exploits this variation across subchannels that occurs in the partial CSI model better than CCSAA. However, for the statistical CSI model, in which these variations are lesser, CCSAA does better than RPA even though it has a weaker performance guarantee. We also observe that the effect of

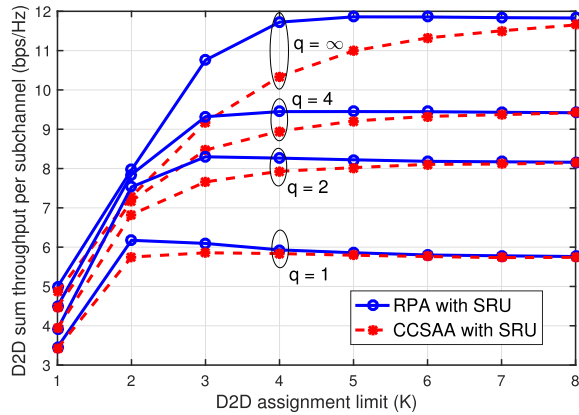


Fig. 6. Partial CSI model: Effect of SRU on the sum throughputs per subchannel of RPA and CCSAA for different  $q$  ( $N = 10$ ,  $M = 30$ , and  $\epsilon_d = 0.1$ ).

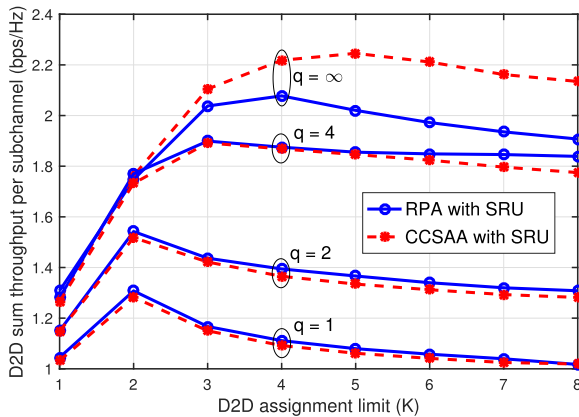


Fig. 7. Statistical CSI model: Effect of SRU on the sum throughputs per subchannel of RPA and CCSAA for different  $q$  ( $N = 10$ ,  $M = 30$ , and  $\epsilon_d = 0.1$ ).

inter-D2D interference is more in the statistical CSI model, which is why the sum throughput is more sensitive to  $K$ . In both models, the sum throughput of RPA is greater than or equal to that of CCSAA when  $K = 1$ .

*Efficacy of SRU:* Fig. 6 plots the sum throughputs per subchannel of RPA and CCSAA with SRU as a function of  $K$  for the partial CSI model. Compared to the results without SRU in Fig. 4, the sum throughputs of both algorithms are now much higher. For example, at  $K = 4$  and  $q = \infty$ , SRU increases the sum throughput of RPA by 65.0% and that of CCSAA by 50.8%. The other trends relative to  $K$  and  $q$  are the same as those in Fig. 4. As before, RPA outperforms CCSAA. The optimal value of  $K$  again depends on  $q$  and is the same as that without SRU.

Fig. 7 plots the corresponding results for the statistical CSI model. Again, SRU markedly improves the sum throughputs of both algorithms. For example, at  $K = 4$  and  $q = \infty$ , SRU increases the sum throughput of RPA by 55.2% and that of CCSAA by 57.8%. Unlike the partial CSI model, the optimal value of  $K$  does change when SRU is used. For RPA, it increases to 3 and 4 for  $q = 4$  and  $\infty$ , respectively. For  $q = 1$  and 2, it remains unchanged. With SRU and  $q = \infty$ ,

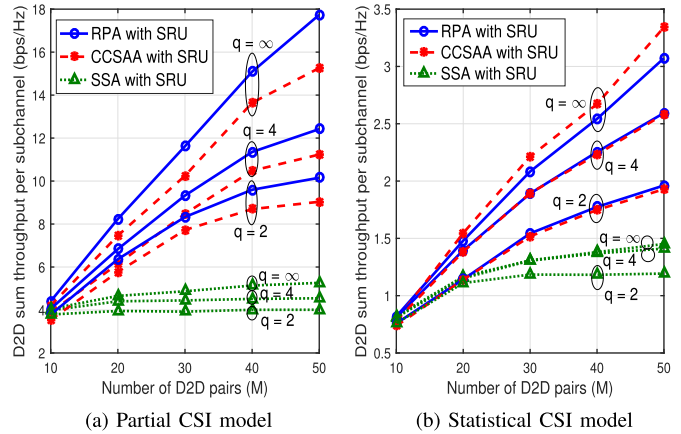


Fig. 8. D2D sum throughputs per subchannel of RPA, CCSAA, and SSA as a function of  $M$  for different  $q$  ( $N = 10$  and  $\epsilon_d = 0.1$ ).

CCSAA outperforms RPA for all  $K \geq 2$ . For  $q = 1, 2$ , and 4, the sum throughput of RPA is marginally higher than that of CCSAA for all  $K$ .

Fig. 8a plots the D2D sum throughputs per subchannel of RPA, CCSAA, and SSA with SRU as a function of the number of D2D pairs  $M$  for the partial CSI model. For every  $M$  and  $q$ , the results for RPA and CCSAA are shown for the optimal value of  $K$ , which is numerically determined. As  $M$  increases, the sum throughputs of RPA and CCSAA increase despite the increase in the inter-D2D interference since the D2D pairs are more closely spaced and more in number both within the cell and also in the neighboring cells. Thus, the two algorithms can scale with  $M$  and can exploit multi-user diversity due to the availability of more D2D pairs. As before, the sum throughputs of all algorithms increase as  $q$  increases. RPA and CCSAA outperform SSA, and the performance gap increases as  $M$  increases because of the increase in the average number of D2D pairs assigned per subchannel, which is equal to  $M/N$ . Also, RPA performs better than CCSAA for all  $M$  and  $q$ . The performance gap increases as  $M$  and  $q$  increases. For example, at  $M = 40$ , the sum throughput of RPA is 8.3% and 10.6% more than that of CCSAA for  $q = 4$  and  $\infty$ , respectively. Fig. 8b plots the corresponding results for the statistical CSI model. The trends with respect to  $q$  are similar to those in Fig. 7. For  $q = \infty$ , CCSAA outperforms RPA. However, for  $q = 2$  and 4, RPA outperforms CCSAA, albeit marginally. The sum throughputs of the two algorithms increase as  $M$  and  $q$  increase and are better than that of SSA.

## V. CONCLUSION

We investigated how assumptions about the CSI of the DTx-to-DRx and CU-to-DRx links affected D2D resource allocation algorithms with different designs and complexities in an underlay D2D system. For the partial and statistical CSI models, we presented a quantized feedback scheme in which the D2D rate achieved from the feedback satisfied a pre-specified probability of outage constraint. For a system with multiple D2D pairs and subchannels, we proposed RPA and CCSAA for assigning at most  $K$  D2D pairs to a subchannel and providing QoS guarantees to the CUs. The two polynomial-time

algorithms offered different trade-offs between performance guarantee and complexity. We also proposed a novel SRU technique that exploited the resource allocation information broadcast by the BS to improve the D2D rates.

Numerically, the sum throughputs of both algorithms were close to that of exhaustive search, and SRU improved them significantly. Inter-D2D interference had a more pronounced effect on the sum throughput for the statistical CSI model than the partial CSI model. RPA outperformed CCSAA for the partial CSI model. However, the numerical trends were quite the opposite for the statistical CSI model even though CCSAA had a weaker performance guarantee. This behavior depended on the variation of the rates across subchannels, which was more for the partial CSI model. The optimal value of  $K$  depended on the algorithm, CSI model, and feedback resolution. In some cases, the benefits of increased spatial reuse outweighed the increase in the inter-D2D interference, making it unnecessary to constrain the number of D2D pairs per subchannel.

## APPENDIX

### A. Proof of Lemma 1

We show feasibility of the D2D pairs allocated to subchannel  $i$  for the following two cases:

1) *When D2D Pair  $k_1$  is Allocated to Subchannel  $i$ :* This assignment is trivially feasible because D2D pair  $k_1$  is not considered for assignment if  $w_{i k_1} > b_i$ , in which case  $x_{i k_1}$  would have been set to 0 initially by RPA.

2) *When D2D Pairs  $k_2, \dots, k_{n_i}$  are Allocated to Subchannel  $i$ :* We express the fractional solution  $\{\tilde{x}_{ij}, j \in \mathcal{D}'_i\}$  of subchannel  $i$  in terms of its virtual subchannels  $i_1, \dots, i_{n_i}$  in the bipartite graph as follows. For  $i_1$ , define  $\tilde{x}_{i_1[1]} \triangleq \tilde{x}_{i[1]}$ ,  $\tilde{x}_{i_1[2]} \triangleq \tilde{x}_{i[2]}, \dots, \tilde{x}_{i_1[j_1-1]} \triangleq \tilde{x}_{i[j_1-1]}$ . The term  $\tilde{x}_{i[j_1]}$  is split into  $\tilde{x}_{i_1[j_1]}$  and  $\tilde{x}_{i_2[j_1]}$  such that  $\sum_{j=1}^{j_1} \tilde{x}_{i_1[j]} = 1$  and  $\tilde{x}_{i_1[j_1]} + \tilde{x}_{i_2[j_1]} = \tilde{x}_{i[j_1]}$ . For  $i_2$ , in addition to  $\tilde{x}_{i_2[j_1]}$ , define  $\tilde{x}_{i_2[j_1+1]} \triangleq \tilde{x}_{i[j_1+1]}$ ,  $\tilde{x}_{i_2[j_1+2]} \triangleq \tilde{x}_{i[j_1+2]}, \dots, \tilde{x}_{i_2[j_2-1]} \triangleq \tilde{x}_{i[j_2-1]}$ . The term  $\tilde{x}_{i[j_2]}$  is split into  $\tilde{x}_{i_2[j_2]}$  and  $\tilde{x}_{i_3[j_2]}$  such that  $\sum_{j=j_1}^{j_2} \tilde{x}_{i_2[j]} = 1$  and  $\tilde{x}_{i_2[j_2]} + \tilde{x}_{i_3[j_2]} = \tilde{x}_{i[j_2]}$ . Note that if  $\sum_{j=1}^{j_1} \tilde{x}_{i[j]} = 1$ , then  $\tilde{x}_{i_2[j_1]} = 0$ . Also, if  $\sum_{j=1}^{j_2} \tilde{x}_{i[j]} = 2$ , then  $\tilde{x}_{i_3[j_2]} = 0$ . In general, for  $k = 1, 2, \dots, n_i$ , define  $\tilde{x}_{i_k[j]} \triangleq \tilde{x}_{i[j]}$  for  $j = j_{k-1} + 1, j_{k-1} + 2, \dots, j_k - 1$ , and  $\tilde{x}_{i[j_k]}$  is split into  $\tilde{x}_{i_k[j_k]}$  and  $\tilde{x}_{i_{k+1}[j_k]}$  such that  $\sum_{j=j_{k-1}}^{j_k} \tilde{x}_{i_k[j]} = 1$  and  $\tilde{x}_{i_k[j_k]} + \tilde{x}_{i_{k+1}[j_k]} = \tilde{x}_{i[j_k]}$ , where  $j_0 \triangleq 1$  and  $\tilde{x}_{i_1[j_0]} \triangleq \tilde{x}_{i[j_0]}$ . Also, if  $\sum_{j=1}^{j_k} \tilde{x}_{i[j]} = k$ , then  $\tilde{x}_{i_{k+1}[j_k]} = 0$ .

For each subchannel  $i$ , the linear program in Step 1 of RPA satisfies (15). Hence,

$$b_i \geq \sum_{j=1}^{|\mathcal{D}'_i|} \tilde{x}_{i[j]} w_{i[j]}. \quad (23)$$

In terms of the notation above, the right hand side of (23) can be expressed as

$$\begin{aligned} & \sum_{j=1}^{|\mathcal{D}'_i|} \tilde{x}_{i[j]} w_{i[j]} \\ &= \tilde{x}_{i_1[1]} w_{i_1[1]} + \tilde{x}_{i_1[2]} w_{i_1[2]} \end{aligned}$$

$$\begin{aligned} & + \dots + (\tilde{x}_{i_1[j_1]} + \tilde{x}_{i_2[j_1]}) w_{i[j_1]} + \tilde{x}_{i_2[j_1+1]} w_{i[j_1+1]} \\ & + \dots + (\tilde{x}_{i_2[j_2]} + \tilde{x}_{i_3[j_2]}) w_{i[j_2]} + \tilde{x}_{i_3[j_2+1]} w_{i[j_2+1]} \\ & + \dots + (\tilde{x}_{i_{n_i-1}[j_{n_i-1}]} + \tilde{x}_{i_{n_i}[j_{n_i-1}]}) w_{i[j_{n_i-1}]} \\ & + \tilde{x}_{i_{n_i}[j_{n_i-1}+1]} w_{i[j_{n_i-1}+1]} + \dots + \tilde{x}_{i_{n_i}[|\mathcal{D}'_i|]} w_{i[|\mathcal{D}'_i|]}. \quad (24) \end{aligned}$$

This can be compactly written as

$$\sum_{j=1}^{|\mathcal{D}'_i|} \tilde{x}_{i[j]} w_{i[j]} = \sum_{k=1}^{n_i-1} \sum_{j=j_{k-1}}^{j_k} \tilde{x}_{i_k[j]} w_{i[j]} + \sum_{j=j_{n_i-1}}^{|\mathcal{D}'_i|} \tilde{x}_{i_{n_i}[j]} w_{i[j]}. \quad (25)$$

Since  $\tilde{x}_{ij} \geq 0$  and  $w_{ij} \geq 0$ , it follows that  $\sum_{j=1}^{|\mathcal{D}'_i|} \tilde{x}_{i[j]} w_{i[j]} \geq \sum_{k=1}^{n_i-1} \sum_{j=j_{k-1}}^{j_k} \tilde{x}_{i_k[j]} w_{i[j]}$ . Since  $w_{i[j_{k-1}]} \geq w_{i[j_{k-1}+1]} \geq \dots \geq w_{i[j_k]}$  (cf. (18)), it follows that

$$\sum_{k=1}^{n_i-1} \sum_{j=j_{k-1}}^{j_k} \tilde{x}_{i_k[j]} w_{i[j]} \geq \sum_{k=1}^{n_i-1} \left( \sum_{j=j_{k-1}}^{j_k} \tilde{x}_{i_k[j]} \right) w_{i[j_k]} = \sum_{k=1}^{n_i-1} w_{i[j_k]}, \quad (26)$$

where the last equality follows because  $\sum_{j=j_{k-1}}^{j_k} \tilde{x}_{i_k[j]} = 1$ , for  $k = 1, \dots, n_i - 1$ . Substituting this in (23), we get

$$b_i \geq w_{i[j_1]} + w_{i[j_2]} + \dots + w_{i[j_{n_i-1}]}. \quad (27)$$

The virtual subchannel  $i_2$  can be assigned to at most one D2D pair among  $[j_1], \dots, k_2, \dots, [j_2]$ , and the maximum interference possible is  $w_{i[j_1]}$ . Hence,  $w_{i[j_1]} \geq w_{i k_2}$ . In general, we can show that  $w_{i[j_1]} \geq w_{i k_2}, w_{i[j_2]} \geq w_{i k_3}, \dots, w_{i[j_{n_i-1}]} \geq w_{i k_{n_i}}$ . Thus, from (27), we get  $b_i \geq w_{i k_2} + w_{i k_3} + \dots + w_{i k_{n_i}}$ . Hence, the set  $\{k_2, k_3, \dots, k_{n_i}\}$  of D2D pairs assigned to subchannel  $i$  is feasible.

### B. Proof of Result 1

Let  $Z_{\text{opt}}$  be the optimal sum rate achievable for  $\mathcal{P}$ , and let  $Z_{\text{frac}}$  be the sum rate obtained by the fractional solution in Step 1 of RPA. Since the fractional solution is obtained by relaxing the integer constraint in (17), it follows that  $Z_{\text{frac}} \geq Z_{\text{opt}}$ . The bipartite graph in Step 2 is the rearrangement of the fractional solution, and the integral matching solution is the optimal one-to-one matching of it when the constraint in (15) is ignored. Let  $Z_{\text{match}}$  be the sum rate obtained by the integral matching solution in Step 3 of RPA. Hence,  $Z_{\text{match}} \geq Z_{\text{frac}}$ . After pruning the infeasible assignment for subchannel  $i$  in Step 4 of RPA, the sum rate achieved is given by  $\max \{C_{i k_1}, C_{i k_2} + \dots + C_{i k_{n_i}}\} \geq (C_{i k_1} + C_{i k_2} + \dots + C_{i k_{n_i}}) / 2$ , which is at least half of the sum rate obtained by the integral matching solution for subchannel  $i$ . Summing over all subchannels, the sum rate  $Z_{\text{final}}$  of the final allocation after pruning satisfies  $Z_{\text{final}} \geq Z_{\text{match}} / 2$ . From the above inequalities, we get  $Z_{\text{final}} \geq Z_{\text{opt}} / 2$ .

## REFERENCES

- [1] B. V. R. Gorantla and N. B. Mehta, "Subchannel allocation with low computational and signaling complexity in 5G D2D networks," in *Proc. IEEE Int. Conf. Commun.*, Montreal, QC, Canada, Jun. 2021, pp. 1–6.
- [2] R. I. Ansari *et al.*, "5G D2D networks: Techniques, challenges, and future prospects," *IEEE Syst. J.*, vol. 12, no. 4, pp. 3970–3984, Dec. 2018.

- [3] O. Maraqa, A. S. Rajasekaran, S. Al-Ahmadi, H. Yanikomeroğlu, and S. M. Sait, "A survey of rate-optimal power domain NOMA with enabling technologies of future wireless networks," *IEEE Commun. Surveys Tuts.*, vol. 22, no. 4, pp. 2192–2235, 4th Quart., 2020.
- [4] D. Feng, L. Lu, Y. Yuan-Wu, G. Y. Li, G. Feng, and S. Li, "Device-to-device communications underlying cellular networks," *IEEE Trans. Commun.*, vol. 61, no. 8, pp. 3541–3551, Aug. 2013.
- [5] T. D. Hoang, L. Le, and T. Le-Ngoc, "Resource allocation for D2D communication underlaid cellular networks using graph-based approach," *IEEE Trans. Wireless Commun.*, vol. 15, no. 10, pp. 7099–7113, Oct. 2016.
- [6] W. Zhao and S. Wang, "Resource sharing scheme for device-to-device communication underlying cellular networks," *IEEE Trans. Commun.*, vol. 63, no. 12, pp. 4838–4848, Oct. 2015.
- [7] R. Zhang *et al.*, "Interference graph-based resource allocation (InGRA) for D2D communications underlying cellular networks," *IEEE Trans. Veh. Technol.*, vol. 64, no. 8, pp. 3844–3850, Aug. 2015.
- [8] H. H. Esmat, M. M. Elmesalawy, and I. I. Ibrahim, "Adaptive resource sharing algorithm for device-to-device communications underlying cellular networks," *IEEE Commun. Lett.*, vol. 20, no. 3, pp. 530–533, Mar. 2016.
- [9] N. Zhao, X. Liu, Y. Chen, Z. Li, B. Chen, and M.-S. Alouini, "Caching D2D connections in small-cell networks," *IEEE Trans. Veh. Technol.*, vol. 67, no. 12, pp. 12326–12338, Dec. 2018.
- [10] D. Feng, L. Lu, Y.-W. Yi, G. Y. Li, G. Feng, and S. Li, "QoS-aware resource allocation for device-to-device communications with channel uncertainty," *IEEE Trans. Veh. Technol.*, vol. 65, no. 8, pp. 6051–6062, Aug. 2016.
- [11] L. Wang, H. Tang, H. Wu, and G. Stüber, "Resource allocation for D2D communications underlay in Rayleigh fading channels," *IEEE Trans. Veh. Technol.*, vol. 66, no. 2, pp. 1159–1170, Feb. 2017.
- [12] S. Bulusu, N. B. Mehta, and S. Kalyanasundaram, "Rate adaptation, scheduling, and mode selection in D2D systems with partial channel knowledge," *IEEE Trans. Wireless Commun.*, vol. 17, no. 2, pp. 1053–1065, Feb. 2018.
- [13] J. Yang, M. Ding, G. Mao, and Z. Lin, "Interference management in in-band D2D underlaid cellular networks," *IEEE Trans. Cognit. Commun. Netw.*, vol. 5, no. 4, pp. 873–885, Dec. 2019.
- [14] A. Ramezani-Kebrya, M. Dong, B. Liang, G. Boudreau, and S. H. Seyedmehdi, "Robust power optimization for device-to-device communication in a multi-cell network under partial CSI," in *Proc. ICC*, Paris, France, May 2017, pp. 1–6.
- [15] R. Li, P. Hong, K. Xue, M. Zhang, and T. Yang, "Energy-efficient resource allocation for high-rate underlay D2D communications with statistical CSI: A one-to-many strategy," *IEEE Trans. Veh. Technol.*, vol. 69, no. 4, pp. 4006–4018, Apr. 2020.
- [16] R. Wang, J. Zhang, S. H. Song, and K. B. Letaief, "Optimal QoS-aware channel assignment in D2D communications with partial CSI," *IEEE Trans. Wireless Commun.*, vol. 15, no. 11, pp. 7594–7609, Aug. 2016.
- [17] D. Verenzuela and G. Miao, "Scalable D2D communications for frequency reuse  $\gg 1$  in 5G," *IEEE Trans. Wireless Commun.*, vol. 16, no. 6, pp. 3435–3447, Jun. 2017.
- [18] B. V. R. Gorantla and N. B. Mehta, "Resource and computationally efficient subchannel allocation for D2D in multi-cell scenarios with partial and asymmetric CSI," *IEEE Trans. Wireless Commun.*, vol. 18, no. 12, pp. 5806–5817, Dec. 2019.
- [19] S. Doumiati, M. Assaad, and H. A. Artail, "A framework of topological interference management and clustering for D2D networks," *IEEE Trans. Commun.*, vol. 67, no. 11, pp. 7856–7871, Nov. 2019.
- [20] A. Memmi, Z. Rezki, and M.-S. Alouini, "Power control for D2D underlay cellular networks with channel uncertainty," *IEEE Trans. Wireless Commun.*, vol. 16, no. 2, pp. 1330–1343, Feb. 2017.
- [21] H. Xu, G. L. Stüber, W. Xu, C. Pan, J. Shi, and M. C. Z. Yang, "Robust transmission design for multicell D2D underlaid cellular networks," *IEEE Trans. Veh. Technol.*, vol. 67, no. 47, pp. 5922–5936, Jul. 2018.
- [22] Y. Hao, Q. Ni, H. Li, and S. Hou, "Robust multi-objective optimization for EE-SE tradeoff in D2D communications underlying heterogeneous networks," *IEEE Trans. Commun.*, vol. 66, no. 10, pp. 4936–4949, Oct. 2018.
- [23] D. B. Shmoys and É. Tardos, "An approximation algorithm for the generalized assignment problem," *Math. Program.*, vol. 62, no. 1, pp. 461–474, Feb. 1993.
- [24] P. Goundan and A. Schulz. (2009). *Revisiting the Greedy Approach to Submodular Set Function Maximization*. [Online]. Available: <http://web.mit.edu/schulz/www/publications.html>
- [25] A. Caprara, H. Kellerer, U. Pferschy, and D. Pisinger, "Approximation algorithms for knapsack problems with cardinality constraints," *Eur. J. Oper. Res.*, vol. 123, no. 2, pp. 333–345, Jun. 2000.
- [26] X. Lin, J. Andrews, A. Ghosh, and R. Ratasuk, "An overview of 3GPP device-to-device proximity services," *IEEE Commun. Mag.*, vol. 52, no. 4, pp. 40–48, Apr. 2014.
- [27] E. Dahlman, S. Parkvall, and J. Skold, *5G NR: The Next Generation Wireless Access Technology*, 1st ed. Cambridge, MA, USA: Academic, 2018.
- [28] H. V. Poor, *An Introduction to Signal Detection Estimation*, 2nd ed. New York, NY, USA: Springer-Verlag, 1994.
- [29] A. J. Izenman, "Recent developments in nonparametric density estimation," *J. Amer. Stat. Assoc.*, vol. 86, no. 413, pp. 205–224, Mar. 1991.
- [30] G. L. Stüber, *Principles of Mobile Communications*, 2nd ed. New Delhi, India: Springer, 2009.
- [31] D. G. Luenberger and Y. Ye, *Linear and Nonlinear Programming*, 3rd ed. New Delhi, India: Springer, 2008.
- [32] D. B. West, *Introduction to Graph Theory*, 2nd ed. Upper Saddle River, NJ, USA: Prentice-Hall, 2000.
- [33] M. W. Best and R. Y. Tan, "An  $O(n^2 \log n)$  strongly polynomial algorithm for quadratic program with two equations and lower & upper bounds," Univ. Waterloo, Waterloo, ON, Canada, Tech. Rep. CORR 90-04, 1990.
- [34] *Technical Specification Group Radio Access Network; Study on Channel Model for Frequencies From 0.5 to 100 GHz (Release 15)*, document 38.901 (v15.0.0), 3GPP, Jun. 2018.



**Bala Venkata Ramulu Gorantla** (Student Member, IEEE) received the Bachelor of Technology degree in electronics and communication engineering from Jawaharlal Nehru Technological University, Hyderabad, in 2006, and the Master of Engineering degree in communication systems from the PSG College of Technology, Coimbatore, in 2009. He is currently pursuing the Ph.D. degree with the Department of Electrical Communication Engineering, Indian Institute of Science, Bengaluru. His research interests include wireless communication, D2D communications, UAV communications, next generation wireless technologies, and optimization.



**Neelesh B. Mehta** (Fellow, IEEE) received the Bachelor of Technology degree in electronics and communications engineering from the Indian Institute of Technology (IIT), Madras, in 1996, and the M.S. and Ph.D. degrees in electrical engineering from the California Institute of Technology, Pasadena, USA, in 1997 and 2001, respectively. He is currently a Professor with the Department of Electrical Communication Engineering, Indian Institute of Science, Bengaluru. He is a fellow of the Indian National Science Academy (INSA), the Indian National Academy of Engineering (INAE), and the National Academy of Sciences India (NASI). He was a recipient of the Shanti Swarup Bhatnagar Award, the Khosla Award, the Vikram Sarabhai Research Award, and the Swarnjayanti Fellowship. He served on the Board of Governor for IEEE ComSoc from 2012 to 2015. He served on the Executive Editorial Committee for the IEEE TRANSACTIONS ON WIRELESS COMMUNICATIONS from 2014 to 2017, and as its Chair from 2017 to 2018. He currently serves as the chair of its steering committee. He has served as an Editor for the IEEE TRANSACTIONS ON COMMUNICATIONS and the IEEE WIRELESS COMMUNICATION LETTERS in the past.